Flame retardant polyphosphoester copolymers as solid polymer electrolyte for lithium batteries

Jorge L. Olmedo-Martínez,[a] Leire Meabe,[b] Raphaël Riva,[c] Gregorio Guzmán-González,[a] Luca Porcarelli,[a,d] Maria Forsyth,[a,d,e] Agurtzane Mugica,[a] Itxaso Calafel,[a] Alejando J. Müller,[a,e] Philippe Lecomte,[c] Christine Jérôme[c] and David Mecerreyes [a,e]

[a]*POLYMAT and Department of Polymers and Advanced Materials: Physics, Chemistry and Technology, Faculty of Chemistry, University of the Basque Country UPV/EHU, Paseo Manuel de Lardizabal 3, Donostia-San Sebastián, Spain*
[b]*SpainCentre for Cooperative Research on Alternative Energies (CIC energiGUNE), Basque Research and Technology Alliance (BRTA), 01510 Vitoria-Gasteiz, Spain*
[c]*Centre for Education and Research on Macromolecules (CERM), CESAM Research Unit, University of Liege (ULiège), Building B6a, 4000 Liège, Belgium*
[d]*ARC Centre of Excellence for Electromaterials Science and Institute for Frontier Materials, Deakin University, Melbourne 3125, Australia*
[e]*IKERBASQUE, Basque Foundation for Science, 48011 Bilbao, Spain*

Abstract

Solid-state lithium batteries are considered one of the most promising battery systems due to their high volumetric energy density and safety. Poly(ethylene oxide) (PEO) is the most commonly used solid polymer electrolyte in solid-state batteries. In this article, we introduce new polyphosphoester polymer electrolytes, which show improved flame retardant properties in comparison with PEO. For this purpose, new polyphosphoester copolymers were synthesized, including phosphoester, poly(ethylene glycol) (PEG) and UV cross-linkable vinyl units. Solid polymer electrolyte films based on polyphosphoester copolymers and lithium bis(trifluoromethanesulfonyl)imide (LiTFSI) were prepared by curing under UV-light. The crystallinity present in the copolymers due to the PEG segment decreases with the amount of salt in the electrolyte, as seen by DSC. Solid polymer electrolytes based on polyphosphoester copolymers show ionic conductivity values as high as 2×10^{-4} S cm^{-1} at 70 °C. FTIR analysis showed that lithium cations complexed with phosphoester groups provoked an increase in the lithium transference number to 0.26 as compared to that of PEO 0.17. Pyrolysis flow combustion calorimetry (PCFC) or micro-calorimetry results demonstrated the improved flame retardancy of the polyphosphoesters in comparison to a reference PEO based polymer electrolyte. The selected polyphosphoester solid electrolyte was investigated in a solid-state lithium cell Li⁰/polymer

electrolyte/LFP battery showing a specific capacity retention close to 80% and coulombic efficiency greater than 98% over 100 cycles at 70 °C.

Introduction

In the XXIst century, a consolidated energy storage system will revolutionize the technology demanded in electric vehicles or in smart grid facilities.[1] Lithium metal batteries with a specific capacity of 3860 mA h g^{-1} could be a competitive candidate to prevail among other battery chemistries. The electrolyte is one of the key components in the performance of the battery. Classic electrolytes are normally based on flammable organic solvents and lithium salts (e.g. 1 M LiPF$_6$-EC/EMC). For this reason, solid-state batteries are seen as the most promising future battery technology in applications where safety is a must, such as in electric vehicles. In this sense, solid polymeric electrolytes (SPEs) composed of polymer as a host matrix of lithium salt have been presented as a safer option due to its low flammability. The gold standard solid polymer electrolyte for lithium battery applications is poly(ethylene oxide) (PEO), owing to its excellent ability to solvate lithium salts.[2,3] The high of ionic conductivity values reached at 70 °C, and good chemical and thermal properties make PEO based solid-state batteries able to run at temperatures >60 °C. However, PEO still shows limitations for batteries that run at room temperature or make use of new generation high voltage cathodes. For this reason, alternative polymer electrolytes to PEO are actively being searched, which offer advantageous properties such as higher ionic conductivity, electrochemical window, or lithium transference number, which allow to improve the performance of Solid-State Batteries. In this respect, little efforts have been devoted in designing polymers to improve the flame retardancy of PEO polymer electrolytes. One of the first options to improve the safety of lithium batteries was to introduce components such as phosphates into the liquid electrolyte,[4,5] but increasing the amount of these compounds in the electrolyte decreased battery performance. Another idea studied was the use of Mg(OH)$_2$ as a separator or in polymer electrolytes. In particular, the use of polymer/Mg (OH)$_2$ systems improved the flame resistance by increasing the hydroxide concentration, and improved the physical adhesion between the electrode and the separator.[6,7]

It is know that the presence of nitrogen or phosphorus atoms in the structure of additives or polymers promotes the carbonization of the polymer on heating and reduces the amount of volatile combustible products.[8] Within the study of flame retardants in polymer electrolytes, trimethyl phosphate has been used as a solvent, which helped to decrease the flammability of electrolytes containing ethylene carbonate (EC) and propylene carbonate (PC).[9] More recently, Xiang et al.[10] proposed the use of 1,3-dioxolane (PDE) polymerized in situ with the addition of tris(pentafluorophenyl)borane (TB) additive, the in situ formation of PDE improved the flame retardant properties and the incorporation of TB contributed to the stabilization of the solid electrolyte interface (SEI). Other examples found in the literature include the use of additives such as pyrrolidinium- and imidazolium-based ionic liquids due to their non flammable/non-volatile property.[11–13]

Polyphosphoesters (PPEs), containing phosphoester bonds in the main chain, are biodegradable and biocompatible, and therefore, their principal application is described in biomedicine, mainly known in drug delivery systems.[14–16] Apart from this, PPEs possess excellent thermal stability, fire resistance, and attractive mechanical properties.[17] In fact, organic flame retardants that contain phosphorus groups have attracted much attention in industrial applications.[18,19] As a representative study, Wang et al., reported a polyphosphonate that shows excellent flame retardancy, which was able to prolongate the time to ignition. A meaningful reduction of the peak heat release rate (HRR) by 57% and a decrease of the specific extinction area was reported.[20] However, the use of polyphosphoesters as SPEs in batteries has been poorly explored. Initial works, reported the synthesis and evaluation of different polyphosphoesters as SPEs, show an ionic conductivity values of $\sim 10^{-6}$ S cm^{-1} at 70 °C, which are very low for practical use of these materials in lithium batteries.[21] The use of phosphonate molecules as flame retardant additives in SPEs has also been reported.[22]

In this article, we synthesized new tailor-made polyphosphoester copolymers and evaluated them as polymer electrolytes for lithium solid state batteries. The new polyphosphoester polymer electrolytes were characterized in terms of thermal and electrochemical properties. Particular attention was paid to investigate the flame retardancy of the polyphosphoester copolymers using pyrolysis flow combustion calorimetry (PCFC) or microcalorimetry. Additionally, the most promising polyphosphoester polymer electrolyte was evaluated in a lithium metal/polyphosphoester/lithium iron phosphate solid state lithium cell through charge–discharge tests. During the discussion of results, PEO used as a reference for being the reference solid polymer electrolyte in lithium batteries nowadays.

Experimental section

MATERIALS

Poly(ethylene glycol) (PEG) (M_w = 4000 g mol^{-1}, Aldrich) was used as received. Toluene (VWR), dichloromethane (CH$_2$Cl$_2$, VWR), benzyl alcohol (Aldrich), and 1,8 diazobicyclo [5.4.0] undec-7-ene (DBU, Aldrich) were dried over calcium hydride at 25 °C, following by distillation under reduced pressure just before use. TU (thiourea) was synthesized according to the method described by Pratt et al.,[23] and dried overnight under vacuum before use. Butenyl phosphate cyclic monomer (BenEP) and butyl phosphate cyclic monomer (BEP) were synthesized following the procedures described by Clement et al.[24] The polymers were synthesized following the procedures described by Vanslambrouck et al.[25] Poly(ethylene oxide) (PEO) (M_v = 100 000 g mol^{-1}, Sigma Aldrich), acetonitrile (ACN), lithium bis(trifluoromethanesulfonyl)imide (LiTFSI) (99.9%, Solvionic), 2-hydroxy-2-methylpropiophenone (DAROCUR 1173) as photoinitiator from Merck.

SYNTHESIS OF POLYPHOSPHOESTER COPOLYMERS

Poly(BEP-co-BenEP)-b-PEG-b-(BEP-co-BenP) block copolymer (P1 and P2). Polyethylene glycol (M_w = 4000 g mol^{-1}) (4 g, 1 mmol for P1 and 2 g, 0.5 mmol for P2) was transferred in a round bottom flask and dried by three azeotropic distillations with anhydrous toluene. BenEP (2.5 g, 13.9 mmol) and BEP (2.5 g, 13.9 mmol) monomers were added in the flask. The mixture is then put under vacuum for 10 min 10 mL of anhydrous dichloromethane were then added under N$_2$ atmosphere. After complete solubilization, the mixture was cooled down to 0 °C, and 0.75 mL (5 mmol) of DBU was finally introduced under a N$_2$ atmosphere with a syringe equipped with a stainless-steel capillary. The polymerization medium was then stirred for 30 min. After concentration of the solution under vacuum, the copolymer was precipitated in cold diethyl ether. After decantation, the recovered copolymer was dissolved in methanol and dialyzed against methanol (MWCO = 3.5 kDa) overnight to remove impurities. After evaporation of methanol under vacuum, the copolymer was collected and characterized by NMR and SEC analyses.

P1 COPOLYMER CHARACTERIZATION

^{1}H NMR (CDCl$_3$) δ = 5.78 ppm (m, 10 H, –CH$_2$–C**H**=CH$_2$), 5.11 ppm (m, 20 H, C**H$_2$**=CH–CH$_2$), 4.25 ppm (m, 120 H, O–C**H$_2$**–C**H$_2$**–O and O–C**H$_2$**–CH$_2$–CH$_2$–CH$_3$ of BenEP + O–C**H$_2$**–C**H$_2$**–O, O–C**H$_2$**–CH$_2$–CH=CH$_2$ of BEP), 3.6 ppm (m, 360 H, O–C**H$_2$**–C**H$_2$**–O PEG), 2.41 ppm (m, 20 H, O–CH$_2$–C**H$_2$**–CH=CH$_2$) 1.62 ppm (m, 20 H, CH$_2$–C**H$_2$**–CH$_2$–CH$_3$), 1.46 ppm (m, 20 H, CH$_2$–CH$_2$–C**H$_2$**–CH$_3$) and 0.92 ppm (t, 30 H, CH$_2$–CH$_2$–CH$_2$–C**H$_3$**).

^{31}P NMR (CDCl$_3$) δ = −1.18 ppm and −1.32 ppm.

M_n (^{1}H NMR) = 7600 g mol^{-1}, Đ = 1.1 (SEC).

P2 COPOLYMER CHARACTERIZATION

^{1}H NMR (CDCl$_3$) δ = 5.78 ppm (m, 22 H, –CH$_2$–C**H**=CH$_2$), 5.11 ppm (m, 44 H, C**H$_2$**=CH–CH$_2$), 4.25 ppm (m, 264 H, O–C**H$_2$**–C**H$_2$**–O and O–C**H$_2$**–CH$_2$–CH$_2$–CH$_3$ of BenEP + O–C**H$_2$**–C**H$_2$**–O, O–C**H$_2$**–CH$_2$–CH=CH$_2$ of BEP), 3.6 ppm (m, 360 H, O–C**H$_2$**–C**H$_2$**–O PEG), 2.41 ppm (m, 44 H, O–CH$_2$–C**H$_2$**–CH=CH$_2$) 1.62 ppm (m, 44 H, CH$_2$–C**H$_2$**–CH$_2$–CH$_3$), 1.46 ppm (m, 44 H, CH$_2$–CH$_2$–C**H$_2$**–CH$_3$) and 0.92 ppm (t, 66 H, CH$_2$–CH$_2$–CH$_2$–C**H$_3$**)

^{31}P NMR (CDCl$_3$) δ = −1.18 ppm and −1.32 ppm.

M_n (^{1}H NMR) = 11 000 g mol^{-1}, Đ = 1.1 (SEC).

POLY(BENEP-CO-BEP) (50 MOL% IN BEP) RANDOM COPOLYMER (P3)

TU (926 mg, 2.5 mmol) was transferred in a round bottom flask and dried by three azeotropic distillations with anhydrous toluene. BenEP (3.5 g, 19.6 mmol) and BEP (3.5 g, 19.6 mmol) monomers were added to the flask. The mix is then put under vacuum for 10 min 10 mL of anhydrous dichloromethane were then added under N$_2$ atmosphere. 2 mL of benzylic alcohol stock solution (5

mmol of benzylic alcohol in 100 mL of anhydrous CH_2Cl_2) (0.1 mmol) was added under a N_2 atmosphere. The mixture was cooled down to 0 °C, and DBU (0.4 mL, 2.8 mmol) was finally introduced under a N_2 atmosphere with a syringe equipped with a stainless-steel capillary. The reaction medium was stirred at 0 °C for 30 min. After concentration of the solution under vacuum, the copolymer was precipitated in cold diethyl ether. After decantation, the recovered copolymer was dissolved in methanol and dialyzed against methanol (MWCO = 1 kDa) overnight in order to remove impurities. After evaporation of methanol under vacuum, the copolymer was collected and characterized by NMR and SEC analyses.

P3 COPOLYMER CHARACTERIZATION

^{1}H NMR (CDCl$_3$) δ = 7.5 (m, 5H, aromatic protons), 5.78 ppm (m, 20 H, –CH$_2$–C**H**=CH$_2$), 5.11 ppm (m, 40 H, C**H$_2$**=CH–CH$_2$), 4.25 ppm (m, 240 H, O–C**H$_2$**–CH$_2$–O and O–C**H$_2$**–CH$_2$–CH$_2$–CH$_3$of BenEP + O–C**H$_2$**–CH$_2$–O, O–C**H$_2$**–CH$_2$–CH=CH$_2$ of BEP), 2.41 ppm (m, 40 H, O–CH$_2$–C**H$_2$**–CH=CH$_2$) 1.62 ppm (m, 40 H, CH$_2$–C**H$_2$**–CH$_2$–CH$_3$), 1.46 ppm (m, 40 H, CH$_2$–CH$_2$–C**H$_2$**–CH$_3$) and 0.92 ppm (t, 60 H, CH$_2$–CH$_2$–CH$_2$–C**H$_3$**).

^{31}P NMR (CDCl$_3$) δ = −1.18 ppm and −1.32 ppm.

M_n (^{1}H NMR) = 7000 g mol^{-1}, Đ = 1.1 (SEC).

ELABORATION OF SOLID POLYMER ELECTROLYTES

SPEs were prepared by a solvent casting method dissolving the polyphosphoester copolymers (0.15 g) and the lithium bis(trifluoromethanesulfonyl)imide (LiTFSI) (15 and 30 wt% respect to the copolymer amount) in ACN (3 mL). The solutions were dried on a silicon mold a room temperature for 24 hours, and after the SPEs were dried under high vacuum at 50 °C during 12 h.

The polyphosphoester named P1 and P3 were crosslinked to produce free-standing films by UV-Light using the next methodology. The crosslinked polymer electrolytes were prepared by dissolving in acetonitrile the copolymer (0.15 g), lithium bis(trifluoromethanesulfonyl)imide (LiTFSI) (15 and 30 wt% respect the copolymer amount), the UV photoinitiator (2-hydroxy-2methyl-propiophenone (1 wt% respect the copolymer amount)) in 3 mL of acetonitrile. The solutions were stirred during 1 h, and they were cast onto a silicon mold. The solvent was evaporated at room temperature and later by applying high vacuum. Finally, the films were passed 3 times from a xenon arc lamp (Helios Italquartz, 45 mW cm^{-2}). Before each experiment, the crosslinked copolymers were dried under vacuum at 50 °C during 24 h. Scheme 2 shows the structure of the crosslinked electrolytes.

CHARACTERIZATION METHODS

Differential scanning calorimetry (DSC). PerkinElmer 8500 DSC equipped with an intracooler III, and calibrated with indium and tin standards was used to determined the thermal transitions of the electrolytes. Samples were measured in an aluminum standard tray using approximately 5 mg of electrolyte. Samples were heated from 25 to 100 °C at 20 °C min^{-1}, held for 3 min to erase the thermal history, then cooled to −60 °C and subsequent heating at 20 °C min^{-1}.

Dynamic mechanic thermal analysis (DMTA). This experiment were performed using a rectanglar samples of crosslinked polyphosphoesters electrolytes (10 × 10 × 5 mm), using a Triton 2000 DMA from Triton Technology in compression mode. The tests were performed at 1 Hz and the heating rate of 4 °C min^{-1} from −100 to 100 °C.

Electrochemical impedance spectroscopy (EIS). Ionic conductivity was estimated by EIS in an Autolab 302N potentiostat/galvanostat (Metrohm AG) at different temperatures (100–25 °C), equipped with a temperature controller (Microcell HC station). The sample was placed between two stainless steel electrodes (surface area = 0.5 cm^2). The Nyquist plots were obtained applying a 10 mV perturbation to open circuit in the frequency range of 100 kHz to 1 Hz.

Fourier transform infrared spectroscopy (FTIR). An infrared spectrometer (Bruker Alpha-P) equipped with an attenuated total reflection (ATR) accessory was used. Spectra were obtained in the range of 4000–400 cm^{-1} with a resolution of 4 cm^{-1}.

Electrochemical studies. Lithium-ion transference number was calculated based on Bruce and Vincent method at 70 °C,[26] using the following equation:

$$t_{Li^+} = \frac{I_s(\Delta V - I_0 R_0)}{I_0(\Delta V - I_s R_s)}$$

where R is the resistance, I is the current and ΔV is the potential applied across the cell (10 mV), the subscripts 0 and s, indicate the initial and steady state values respectively. The polymer electrolytes were placed between two lithium electrodes and closed in CR2032. Before the analysis, the cells were left to stabilize at 70 °C for 24 h.

Lithium iron phosphate (LFP) cathode composed by 60 wt% of active material, 10 wt% of conductive carbon (C65) and 30 wt% of copolymer P1 was prepared in a water based slurry. The slurry was cast on aluminum foil and heated at 100 °C to remove the solvent, the loading mass of the active material in the electrodes was ~3 mg cm^{-2}. The Li^0/polymer electrolyte/LFP cells were assembled in the argon filled glove box. The galvanostatic charge–discharge studies were performed using a Biologic VMP-3 battery testing system at 70 °C inside an oven (Thermoscientific). These cells were subjected to three cycles for Solid Electrolyte Inteface (SEI) at a rate of C/10 and then charged and discharged with a constant C-rate of C/10 for constant cycling, and the corresponding charge/ discharge voltage range was between 2.5 and 4 V. The electrochemical characterization was performed in recently assembled cells and subjected at 2 h of stabilization.

Micro calorimeter test. Micro calorimetry measurements were performed using a pyrolysis combustion flow calorimeter (PCFC) Fire Testing Technology FAA microcalorimeter. The mass of the sample was ≈5 mg, the experimental conditions were: a heating rate of 1 K s^{-1}, the specimen temperature was raised up to 700 °C, a combined gas flow rate of 100 cm^3 min^{-1}, an oxygen concentration of 20% O_2 v/v in the combustor, and a combustor temperature of 900 °C. The results were obtained after averaging three samples. Heat release capacity (HRC) and heat released rate (HRR) were calculated based on the oxygen consumption, heating rate, flow rate and sample weigth.[27]

Results and discussion

SOLID POLYMER ELECTROLYTES BASED IN POLYPHOSPHOESTER COPOLYMERS BY UV-CURING

In this work, three different polyphosphoester copolymers were synthesized according to the procedure described by Vanslambrouck et al.[25] Scheme 1 shows the chemical structure of the polyphosphoester copolymers, which were designed to include PEG segments, polyphosphester groups and vinyl functional groups. The PEG segments are known to be the best groups for solvating salt in polymer electrolytes. In addition, the phosphoesters functionalities are expected to improve the flame retardancy. Since polyphosphoesters are typically low T_g polymers which are viscous liquids at room temperature, we choose to add some vinyl functionalities to be able to crosslink the polyphosphoesters copolymers and thus obtain solid-free standing films. Thus, two triblock copolymers (P1 and P2) with a central block of PEG and two lateral blocks made of hydrophobic polyphosphoesters containing 50 mol% of unsaturated pendant group were synthesized. The difference between P1 and P2 copolymers relies on the number of phosphoester subunits in the lateral blocks. A third copolymer exclusively made of polyphosphoester was also prepared as polymer reference without PEG sequence (P3). Scheme 2 shows the typical UV-curing of one polyphosphoester copolymers in the presence of LiTFSI salt and a photoinitiator. As a result of the cross-linking of the initial liquid like low T_g polyphosphoester a free-standing solid polyphosphoester film including LiTFSI was obtained as shown in the picture, Scheme 2.

Scheme 1 *Chemical structure of the three different polyphosphoester copolymers investigated in this work.*

P1 M_n = 7,600 g /mol

P2 M_n = 11,000 g /mol

P3 M_n = 7,000 g /mol
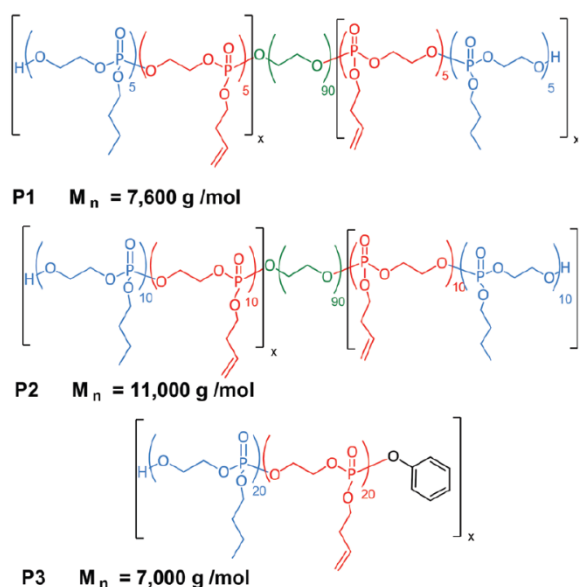
Scheme 2 *Schematic representation of the ultraviolet curing of the polyphosphoester copolymers.*
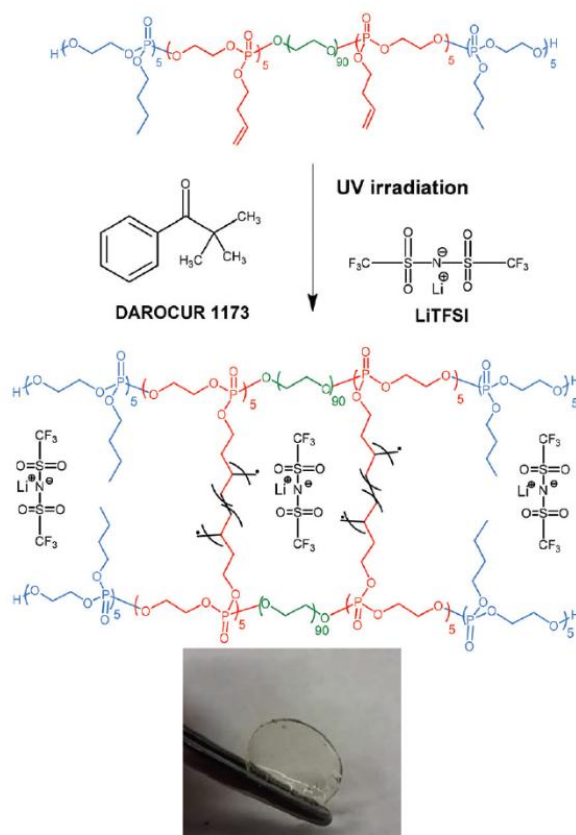
DIFFERENTIAL SCANNING CALORIMETRY (DSC)

It is well known that for the design of new SPEs, amorphous polymers with a low glass transition temperature (T_g) are preferred due to favorable segmental motion for improved ionic conductivity.[28] For this reason, the thermal properties of synthesized PPE-SPEs were evaluated by DSC. Fig. 1 shows the DSC results for the different copolymers, and the corresponding blends; non-crosslinked and crosslinked systems with 15 and 30 wt% LiTFSI. In the neat synthesized polymers two different thermal behavior have been analyzed, P1 and P2 are semicrystalline materials, instead, P3 is an amorphous copolymer.

The melting enthalpy (ΔH_m) values for the copolymers P1 and P2 are respectively 72 and 53 J g^{-1}, which represents 34 and 25% crystallinity degree, which decreases further with the addition of Li salt until the material is completely amorphous. The semi-crystallinity of the P1 and P2 is derived from the presence of the polyethylene oxide block, where the analyzed melting temperature (T_m) in both cases is around 40 °C. However, the molecular weight of the PEG block in the copolymers is 4000 g mol^{-1} and the T_m values are lower than those reported for PEG of this molecular weight (∼55 °C (ref. 29 and 30)). This lowering of T_m can be associated to the introduction of another block, phosphoester group, where the PEG crystallization is hindered and restricted.[31] Moreover, the addition of LiTFSI to these copolymer matrixes, results in a decrease of the T_m, increasing the amorphous phase, Fig. 1a and b. As it can be

observed in Fig. 1a, the T_m in P1 decreases with 15 wt% LiTFSI from 43 °C to 35 °C, and when the electrolyte is crosslinked, following a similar trend, the T_m decreases to 33 °C. Beyond, when 30 wt% LiTFSI is added to the SPEs, P1 and P2 become completely amorphous polymers, with a glass transition temperature (T_g) of −43 and −48 °C, respectively.

Fig. 1c shows the DSC heating scans of P3 copolymer, where it can be corroborated that P3 is completely amorphous owing to the lack of EG units in the polymer. Non-crosslinked and crosslinked electrolytes are completely amorphous and, in all cases the T_g values are as low as around −45 °C without major variation.

Fig. 1 *DSC heating scans of the different polyphosphoester with LiTFSI.*
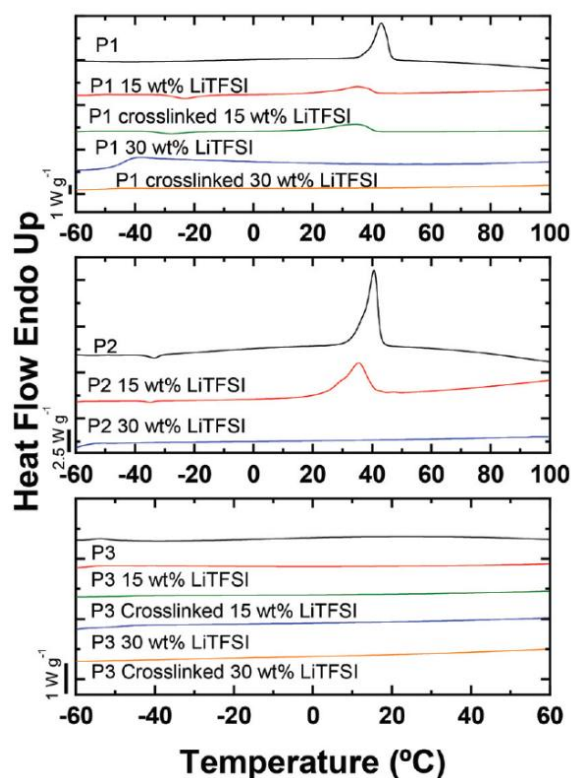
DYNAMIC MECHANICAL THERMAL ANALYSIS (DMTA)

Fig. 2 shows the DMTA results of the P1 copolymer crosslinked and the electrolytes of this copolymer crosslinked with 15 and 30 wt% LiTFSI. DMTA was performed for the crosslinked polymers since the polymers not crosslinked with LiTFSI were viscous liquids, to which this experiment could not be performed. The graph presents the modulus value as a function of temperature, at low temperatures the polymers are in a glassy state,[32] and the storage modulus E', is constant from −100 to −40 °C, where the modulus decreases as the T_g of the polymer passes, these results corroborate those presented by DSC. In the case of crosslinked P1 without LiTFSI, there is another drop in the modulus which is attributed to a fusion of the part containing PEG segments, in the case of electrolytes the T_g at −40 °C is observed and the modulus decreases as a function of the salt concentration in the system, even so,

the values of the modulus at 70 °C, 1.56×10^6 Pa with 15 wt% LiTFSI and 6.6×10^5 Pa with 30 wt% LiTFSI, are comparable with other values reported in the literature.[33–35]

MICROCALORIMETER CHARACTERIZATION

A microcalorimeter is a bench-scale instrument used to determine the flammability parameters of materials under laboratory conditions. The more important parameters are the heat release rate (HRR) and peak heat release rate (PHRR). Fig. 3 shows these parameters as a function of time and temperature. The thermal stability of the polymers was also observed by TGA (ESI, Fig. S2†), and it is observed that the decomposition temperature (T_d) of the polymer shows a similar trend compared to PHRR values obtained in the microcalorimeter runs (Table 1). Combustibility depends as much on fire conditions as on polymer composition,[36] in this case, the PEO was taken as a reference, since the copolymer P1 has a PEG block in its chemical structure. The behavior of the temperature at peak heat release rate (PHRR) in the graphs (Fig. 3a) shows that the PEO needs above 400 °C for this material to catch fire, when adding LiTFSI to the PEO this temperature is a bit higher, but they are the ones that need the least time for ignition. In the case of materials with phosphoester groups, the temperature necessary for ignition is 328 °C and decreases when adding lithium salt, but the fire-retardant property is observed in Fig. 3b, where it is necessary a longer time for ignition.

Table 1 shows the quantitative results obtained by this technique: it is observed that the following parameters; the heat release capacity (HRC), which is related to the fire hazard of the material and total heat release (THR), which is the amount of heat released throughout the decomposition, decrease when LiTFSI is added, and at the same time these values are lower in the electrolytes based on the copolymers, which proves that flammability of these materials is decreased.

Fig. 2 *DMTA of crosslinked polyphosphoester polymer electrolytes.*
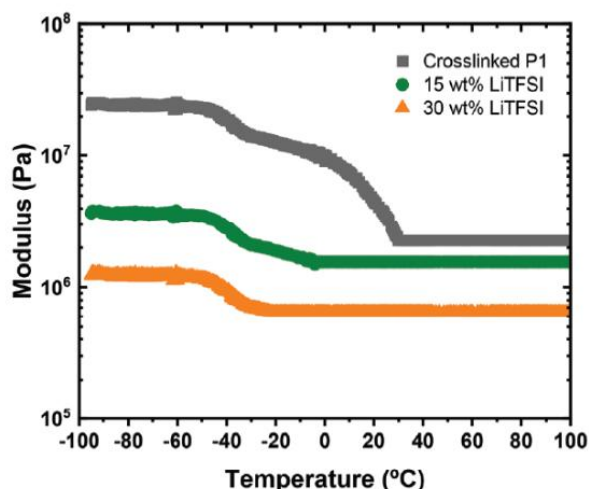
Fig. 3 *Microcalorimeter test as a function of (a) temperature, (b) time.*
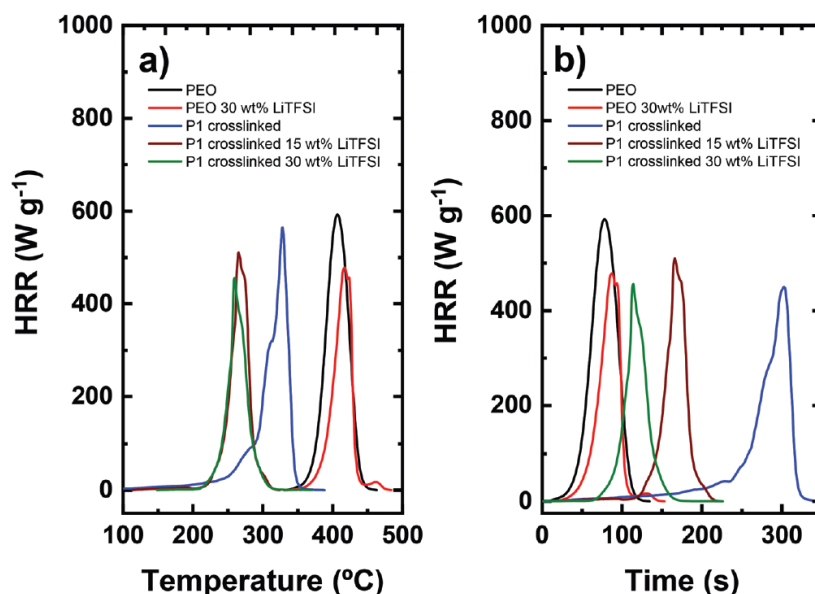
Table 1 *Micro calorimeter data*

Sample	HRC (J g^{-1} K^{-1})	Peak HRR (W g^{-1})	Total HR (KJ g^{-1})	T_p (°C)	$T_d{}^a$ (°C)
PEO	600	592.91	23.90	406.74	387
PEO 30 wt% LiTFSI	544.68	545.26	16.07	421.1	416
P1 crosslinked	418.4	420.12	20.57	324.57	298
P1 crosslinked 15 wt% LiTFSI	525.2	525.5	16.32	265.8	265
P1 crosslinked 30 wt% LiTFSI	459.93	449.09	14.44	259.32	259

^{a} Decomposition temperature (T_d) obtained by TGA.

IONIC CONDUCTIVITY AND LI-ION TRANSFERENCE NUMBER ($T_{Li}{}^+$)

Next, the ionic conductivity of the prepared SPEs was evaluated. Fig. 4 shows the ionic conductivity as a function of temperature for the different non-crosslinked SPEs. In the ionic conductivity experiments, PEO was used as a reference. Fig. 4a shows the behavior of ionic conductivity of all copolymers and PEO with 15 wt% LiTFSI. The behavior is directly related to the amount of ethylene oxide units in the polymer structure; the ionic conductivity decreases with the increase in phosphoester concentration in the copolymer (PEO > P1 > P2 > P3). In addition, PEO, P1 and P2 with 15 wt% of salt present some crystallinity as shown in the DSC results (Fig. 1), but being such a low crystallinity, the drop in ionic conductivity values is not appreciated. In the case of P3, as it is completely amorphous, no drop is evidenced with the temperature decrease.

Fig. 4b shows the ionic conductivity data corresponding to the SPEs with 30 wt% LiTFSI. All SPEs are amorphous and provide a superior ionic conductivity with respect to that of the 15 wt% LiTFSI-SPEs.

The same behavior occurs with SPEs containing 15 wt% LiTFSI, the highest values of ionic conductivity are obtained with PEO, and the newly developed polymers follow the same tendency as in 15 wt% LiTFSI-SPEs, *i.e.*, P1 > P2 > P3. All in all, P1–30 wt% LiTFSI offers the remarkable high ionic conductivity value among the synthesized polymers, 5×10^{-4} S cm^{-1} at 70 °C and 3×10^{-5} S cm^{-1} at 25 °C.

Among the synthesized copolymers P1 and P3 are selected to improve the mechanical properties in order to further evaluate the effect of phosphoester groups. Fig. 4c and d represent the ionic conductivity comparison of non-crosslinked and UVcrosslinked P1 and P3 materials, Fig. 3c shows the electrolytes with 15 wt% LiTFSI, whereas Fig. 4d, the electrolytes with 30 wt% LiTFSI. The ionic conductivity values slightly decrease when the polymer is crosslinked, as the polymer structure becomes more rigid, which is also evidenced in the DSCs, where the T_g of the crosslinked electrolytes is slightly higher, Fig. 1. Nevertheless, a compromised balance between good mechanical properties and a good ionic conductivity have been succeeded with UV-crosslinked polymer P1 30 wt% LiTFSI: 2×10^{-4} S cm^{-1} at 70 °C and 1.9×10^{-5} S cm^{-1} at 25 °C.

The lithium transference number (t_{Li}^+) is calculated using the Bruce and Vincent method[26](Fig. 5). The Li-ion transference number at 70 °C for this electrolyte is 0.26. This value is slightly higher compared to PEO-based SPE with 30 wt% LiTFSI, which is close to 0.17.[37] The increase in the number of lithium transport could be due to the fact that there are new complexing groups in the polymer, such as –P=O groups, as suggested in FTIR analysis, (in the next section will be evaluated). To the same extent that has been studied in other polymer chemistries (*e.g.* polycarbonates[38,39] or polyesters[40]) the coordination between P=O and lithium cation could be weaker than EG units, and therefore, the lithium mobility is promoted.

Fig. 4 *Ionic conductivity of PEO and polyphosphoester copolymers, (a) with 15 wt% LiTFSI, (b) with 30 wt% LiTFSI, (c) P1 and P3 crosslinked with 15 wt% LiTFSI and (d) P1 and P3 crosslinked with 30 wt% LiTFSI.*
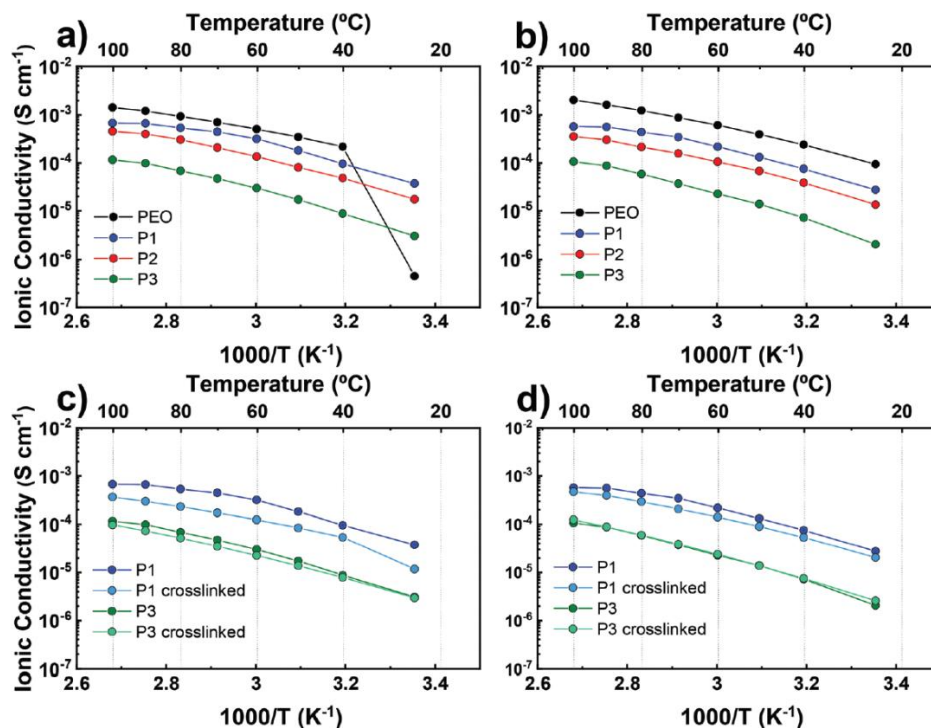
FOURIER TRANSFORM INFRARED SPECTROMETRY (FTIR) ANALYSIS

FTIR spectrum of electrolytes provides information on how LiTFSI cations and anions are complexed in the host polymer. Generally, the lithium ions are solvated by EG units in the polymer backbone of PEO-SPEs.[41,42] The study of coordination environments is evaluated for non-crosslinked P1 and P3 copolymers. Even if P1 copolymer, provides the most promising ionic conductivity, for an easier evaluation of the role of phosphoester groups in the matrix, P3 copolymer is included in this study, where there is no PEG block in the polymer structure. Fig. S3a† displays the FTIR spectra for P1 based SPEs, whereas Fig. S3b† corresponds to P3 based SPEs. In both cases two LiTFSI concentrations are evaluated: 15 and 30 wt% LiTFSI.

The study of FTIR range is focused between 1400–900 cm^{-1}, being the range in which the possible coordination vibration of salt with the phosphoester groups is expected. In P1, the bands that correspond to P–O–C (1060 cm^{-1}) and PvO (1277 cm^{-1}) are slightly shifted to lower wavenumbers, which might be attributed to the coordination bond formed between oxygen atoms from ether group and phosphate and lithium ion. This indicates the favorable interaction between the lithium ions and the copolymers. The bands that correspond to TFSI$^-$ anion are also represented in the FTIR spectra range. The asymmetric S–N–S stretching mode[43] in non-coordinating environment, appears in 1059 cm^{-1}, whereas when the TFSI anion is presented in ion aggregates, the vibrations is shifted 1140 and 1197 cm^{-1}.[44] The vibration in 1324 and 1345 cm^{-1} correspond to C–SO$_2$–N bonding mode,[45,46] 1197 cm^{-1} is the symmetric stretching mode of CF$_3$,[47] 1243 cm^{-1} that correspond to asymmetric SO$_3$ vibrations.[47] Also, the bands 1243, 1324 and 1345 cm^{-1} represent the contact ion pair Li$^+$TFSI$^-$.[44] Due to the intensity and the wavenumber of the peaks, it can be said that most of the TFSI anions are in clusters.

Fig. 5 *ac- and dc-measurements for the lithium ion transference number measurements crosslinked P1 30 wt% LiTFSI electrolyte.*
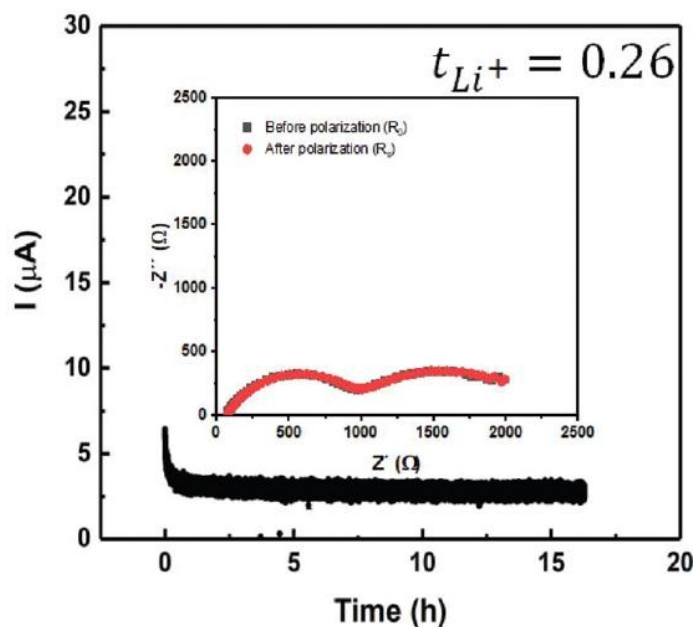
BATTERY TEST

Owing to the ionic conductivity of UV-crosslinked P1 shown at 70 °C, 2×10^{-4} S cm^{-1} and its improved flame retardancy this copolymer was chosen to be investigated in solid state batteries. An important difference between using liquid electrolytes and SPEs is the contact between the electrolyte and the electrode, whereas when using a liquid electrolyte, all the pores of the electrode are filled with electrolyte facilitating the transport of charge, while in solid state batteries, conduction is more difficult in the cathode. For this reason, P1/LiTFSI was also chosen to use as binder, to ensure ionic conduction within the porous structure of the cathode and crosslinked P1 30 wt% LiTFSI as solid polymer electrolyte. The lithium/polyphosphoester/lithium iron phosphate cell (Fig. 6) was tested at a C-rate of C/10 between 4 and 2.5 V at 70 °C. The decrease in the first few cycles can be explained by the sequestration of lithium ions, possibly due to the formation of a passivation layer at the electrode/electrolyte interface.[48]

Even if a capacity drop can be observed among the cycles, 112 mA h g^{-1} in the 1st cycles, 74 mA h g^{-1} in the 100th cycle (71.8% and 47.5% of the theoretical value with respect to LiFePO$_4$ cathode), good efficiencies (>98%) have been disclosed, that confirms the reversibility of the lithium ion intercalation process as well as the electrochemical stability of the polyphosphoester copolymer electrolyte. Even if cell composition can be optimized for an improved battery performance these results indicate the good efficiency of the battery using this cathode composition and electrolyte.

Fig. 6 *Specific capacity versus cycle number profile of the Li/crosslinked P1 30 wt% LiTFSI/LiFePO4 cell at 70 °C.*
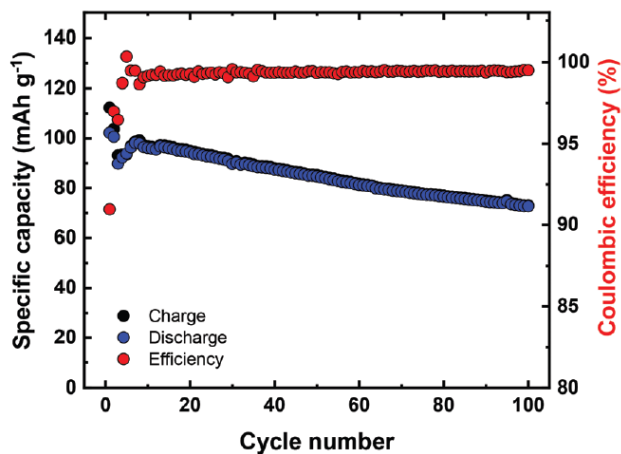
Conclusions

Three different polyphosphoester-based copolymers were successfully synthesized, two triblock copolymers with a central PEG segment and one random copolymer only composed of polyphosphoester to be studied as solid polymer electrolytes for lithium batteries. The crystallinity of the copolymers having a PEG central segment decreases with the incorporation of LiTFSI, and the ionic conductivity in these electrolytes is slightly lower than the PEO reference system. The presence of PEG

segments positively affects the ionic conductivity, the conductivity found at 70 °C for the copolymer P1 with 30 wt% LiTFSI was equal to 2×10^{-4} S cm^{-1}. By FTIR, it was concluded that lithium cations also complexed with phosphoester groups, which caused a slight increase in the number of lithium transfer, obtaining a value of 0.26, which is higher than that of the PEO/LiTFSI system. The lithium/polyphosphoester/LiFePO$_4$ cell based on synthesized P1 copolymer with 30 wt% LiTFSI, maintains a coulombic efficiency greater than 98% with specific capacity values that decrease a little with the number of cycles. Interestingly, the fire resistance of these electrolytes was tested, and it was observed that the presence of phosphoester groups acts as flame retardant, which may help for the safety of the batteries devices.

Author contributions

The manuscript was written through contributions of all authors. Conceptualization: David Mecerreyes. Investigation: Jorge L. Olmedo-Martínez, Leire Meabe, Raphaël Riva, Luca Porcarelli. Data curation: Jorge L. Olmedo Martínez, Gregorio Guzmán-González and Luca Porcarelli. Supervision: David Mecerreyes, Alejandro J. Müller. Validation: Gregorio GuzmánGonzález, Maria Forsyth, Agurtzane Mugica, Alejandro J. Müller, Philippe Lecomte, Christine Jérôme and David Mecerreyes. Writing-original draft-: Jorge L. Olmedo Martínez, Leire Meabe. Writing-review and editing-: David Mecerreyes and Alejandro J. Müller.

Conflicts of interest

There are no conflicts to declare.

Acknowledgements

†Electronic supplementary information (ESI) available: 1. FTIR of P2 with different salt concentration. 2. TGA plot of crosslinked electrolytes. See DOI:10.1039/d1py00344e

References

1. M. Forsyth, L. Porcarelli, X. Wang, N. Goujon and D. Mecerreyes, *Acc. Chem. Res.*, 2019, 52, 686–694.

2. J. Mindemark, M. J. Lacey, T. Bowden and D. Brandell, *Prog. Polym. Sci.*, 2018, 81, 114–143.

3. P. Barai, K. Higa and V. Srinivasan, *Phys. Chem. Chem. Phys.*, 2017, 19, 20493–20505.

4. H. F. Xiang, H. Y. Xu, Z. Z. Wang and C. H. Chen, *J. Power Sources*, 2007, 173, 562–564.

5. Y. E. Hyung, D. R. Vissers and K. Amine, *J. Power Sources*, 2003, 119, 383–387.

6. A. Stephan, *Eur. Polym. J.*, 2006, 42, 21–42.

7. S. Kim, T. Han, J. Jeong, H. Lee, M.-H. Ryou and Y. M. Lee, *Electrochim. Acta*, 2017, 241, 553–559.

8. M. Le Bras, S. Bourbigot, G. Camino and R. Delobel, *Fire retardancy of polymers: the use of intumescence*, Elsevier, 1998, vol. 224.

9. X. Wang, E. Yasukawa and S. Kasuya, *J. Electrochem. Soc.*, 2001, 148, A1058.

10. J. Xiang, Y. Zhang, B. Zhang, L. Yuan, X. Liu, Z. Cheng, Y. Yang, X. Zhang, Z. Li and Y. Shen, *Energy Environ. Sci.*, 2021, DOI: 10.1039/D1EE00049G.

11. P.-L. Kuo, C.-H. Tsao, C.-H. Hsu, S.-T. Chen and H.-M. Hsu, *J. Membr. Sci.*, 2016, 499, 462–469.

12. D. R. MacFarlane, N. Tachikawa, M. Forsyth, J. M. Pringle, P. C. Howlett, G. D. Elliott, J. H. Davis, M. Watanabe, P. Simon and C. A. Angell, *Energy Environ. Sci.*, 2014, 7, 232–250.

13. S. B. Kale, T. C. Nirmale, N. D. Khupse, B. B. Kale, M. V. Kulkarni, S. Pavitran and S. W. Gosavi, *ACS Sustainable Chem. Eng.*, 2021, 9, 1559–1567.

14. T. Steinbach and F. R. Wurm, *Angew. Chem., Int. Ed.*, 2015, 54, 6098–6108.

15. K. N. Bauer, H. T. Tee, M. M. Velencoso and F. R. Wurm, *Prog. Polym. Sci.*, 2017, 61–122.

16. Z. E. Yilmaz and C. Jérôme, *Macromol. Biosci.*, 2016, 16, 1745–1761.

17. K. D. Troev, *Polyphosphoesters: Chemistry and Application*, 2012.

18. C. Zhang, T. F. Garrison, S. A. Madbouly and M. R. Kessler, *Prog. Polym. Sci.*, 2017, 91–143.

19. A B. Morgan and J. W. Gilman, *Fire Mater.*, 2013, 259–279.

20. H. O. Pastore, A. Frache, E. Boccaleri, L. Marchese and G. Camino, *Macromol. Mater. Eng.*, 2004, 289, 783–786.

21. S. Iliescu, N. Plesu and G. Ilia, in *Pure and Applied Chemistry*, 2016, pp. 941–952.

22. M. F. Rectenwald, J. R. Gaffen, A. L. Rheingold, A. B. Morgan and J. D. Protasiewicz, *Angew. Chem.*, 2014, 126, 4257–4260.

23. R. C. Pratt, B. G. G. Lohmeijer, D. A. Long, N. P. Lundberg, A. P. Dove, H. Li, C. G. Wade, R. M. Waymouth and J. L. Hedrick, *Macromolecules*, 2006, 39, 7863–7871.

24. B. Clement, B. Grignard, L. Koole, C. Jerome and Lecomte, *Macromolecules*, 2012, 45, 4476–4486.

25. S. Vanslambrouck, B. Clement, R. Riva, L. H. Koole, D. G. M. Molin, G. Broze, P. Lecomte and C. Jérôme, *RSC Adv.*, 2015, 5, 27330–27337.

26. J. Evans, C. A. Vincent and P. G. Bruce, *Polymer*, 1987, 28, 2324–2328.

27. R. E. Lyon and R. N. Walters, *J. Anal. Appl. Pyrolysis*, 2004, 71, 27–46.

28. D. Devaux, L. Liénafa, E. Beaudoin, S. Maria, T. N. T. Phan, D. Gigmes, E. Giroud, P. Davidson and R. Bouchet, *Electrochim. Acta*, 2018, 269, 250–261.

29. D. Fischer, *Polym. Cryst.*, 2020, 3, e10153.

30 *L. Mandelkern, Crystallization of Polymers, Cambridge University Press, Cambridge, United Kingdom, 2nd ed., 2002.*

31 *H. Schmalz, A. Knoll, A. J. Müller and V. Abetz, Macromolecules, 2002, 35, 10004–10013.*

32 *A. Shaplov, L. Goujon, F. Vidal, E. I. Lozinskaya, F. Meyer, I. A. Malyshkina, C. Chevrot, D. Teyssié, I. L. Odinets and Y. S. Vygodskii, J. Polym. Sci., Part A: Polym. Chem., 2009, 47, 4245–4266.*

33 *M. Álvarez Tirado, L. Castro, G. Guzmán-González, L. Porcarelli and D. Mecerreyes, ACS Appl. Energy Mater., 2021, 4, 295–302.*

34 *J. Shim, L. Kim, H. J. Kim, D. Jeong, J. H. Lee and J.-C. Lee, Polymer, 2017, 122, 222–231.*

35 *P. Sutton, M. Airoldi, L. Porcarelli, J. L. Olmedo-Martínez, C. Mugemana, N. Bruns, D. Mecerreyes, U. Steiner and Gunkel, Polymers, 2020, 12, 595.*

36 *C. Markwart, A. Battig, T. Kuckhoff, B. Schartel and F. R. Wurm, Polym. Chem., 2019, 10, 5920–5930.*

37 *K. Pożyczka, M. Marzantowicz, J. R. Dygas and F. Krok, Electrochim. Acta, 2017, 227, 127–135.*

38 *B. Sun, J. Mindemark, K. Edström and D. Brandell, Solid State Ionics, 2014, 262, 738–742.*

39 *Meabe, T. V. Huynh, N. Lago, H. Sardon, C. Li, L. A. O'Dell, M. Armand, M. Forsyth and D. Mecerreyes, Electrochim. Acta, 2018, 264, 367–375.*

40 *Meabe, S. R. Peña, M. Martinez-Ibañez, Y. Zhang, E. Lobato, H. Manzano, M. Armand, J. Carrasco and H. Zhang, J. Phys. Chem. C, 2020, 124, 17981–17991.*

41 *D. Devaux, R. Bouchet, D. Glé and R. Denoyel, Solid State Ionics, 2012, 227, 119–127.*

42 *Piszcz, O. Garcia-Calvo, U. Oteo, J. M. Lopez del Amo, C. Li, L. M. Rodriguez-Martinez, H. Ben Youcef, N. Lago, J. Thielen and M. Armand, Electrochim. Acta, 2017, 255, 48–54.*

43 *S. Ahmad, H. B. Bohidar, S. Ahmad and S. A. Agnihotry, Polymer, 2006, 47, 3583–3590.*

44 *D. Hambali, Z. Osman, L. Othman, K. B. M. Isa and Harudin, J. Polym. Res., 2020, 27, 1–12.*

45 *R. Kumar, J. P. Sharma and S. S. Sekhon, Eur. Polym. J., 2005, 41, 2718–2725.*

46 *S. Ramesh and C. W. Liew, Measurement, 2013, 46, 1650–1656.*

47 *S. Ramesh, K. H. Leen, K. Kumutha and A. K. Arof, Spectrochim. Acta, Part A, 2007, 66, 1237–1242.*

48 *L. Porcarelli, A. S. Shaplov, M. Salsamendi, J. R. Nair, Y. S. Vygodskii, D. Mecerreyes and C. Gerbaldi, ACS Appl. Mater. Interfaces, 2016, 8, 10350–10359.*